Nature of Surface Sulfate Species and the Generation of Active Sites on Silica−Zirconia Mixed-Oxide Catalysts

Daniel J. Rosenberg, Belén Bachiller-Baeza, Trevor J. Dines, and James A. Anderson*

Surface Chemistry and Catalysis Group, Division of Physical and Inorganic Chemistry, The University, Dundee DD1 4HN, Scotland, U.K.

Received: January 23, 2003

Two series of sulfated silica−zirconia mixed oxides have been prepared and the densities of both Brønsted and Lewis acid sites calculated. Catalytic activity data were obtained for two Brønsted acid catalyzed reactions, the alkylation of toluene by styrene in the liquid phase and but-1-ene double bond isomerization in the gas phase, but no correlation could be obtained between activity and the number of Brønsted acid sites available. Using ab initio calculations for the sulfate structures and the determination of molar absorption coefficients for adsorbed pyridine which was used as a probe for both types of acid site, an understanding of the evolution of acid site densities as a function of sulfate loading has been established. Using this information, it is proposed that the active site for these reactions, which both involve a step involving protonation of the C═C group, must involve an adjacent Brønsted and Lewis acid site pair where the latter acts to initially adsorb the vinyl group prior to protonation.

Introduction

Acid catalysts are widely used in industry to catalyze reactions including isomerizations, alkylations, and catalytic reforming of alkanes. They are also being introduced into highly selective chemical and fine chemical synthesis. There are increasing demands for the use of solid acids to replace inorganic liquid acids. The former include zeolites, heteropoly acids, and oxides, either as single component or as a mixture of two or more components. One method of modifying the acid properties of a solid oxide is by use of dopant ions, with sulfate being one of the mostly widely used. The enhanced, possibly superacidic, catalytic properties resulting from sulfate addition have been most widely studied for zirconia.[1−3] It is known that the final acid properties of the sulfated zirconia materials have a crucial dependence on three principle preparative parameters: the calcination temperature of the nonsulfated zirconia precursor, the surface sulfate concentrations, and the in-situ thermal activation of the sulfated zirconia.[1,4,5] These parameters influence the density of sulfate groups, the oxide phase which is present, and the degree of hydration of the surface active sulfate. Several models have been proposed regarding the structure of the sulfate group to account for the presence of both Brønsted and Lewis acid sites on sulfated zirconia.[3−10] The influence of sulfate on the acidic properties of silica containing mixed oxides has also been reported.[7,11−14] When preparing these mixed oxides, sulfation is often achieved via wet impregnation where the mixed oxide is contacted with an aqueous solution of sulfuric acid. When a mixed oxide is sulfated in such a manner, the sulfur containing species are thought to be exclusively associated with the non-silica component of the mixed oxide.[15] However, this method may induce segregation at the surface of silica-containing mixed oxides[11,13,16] as a result of hydrolysis of the Si−O−M bonds, leading to extraction of the M cation and formation of amorphous sulfated oxide deposited on silica. A sulfated silica−zirconia mixed oxide may therefore be thought of as sulfated zirconia dispersed within a silica lattice. This has the advantage of permitting a degree of control over the particular phase of zirconia formed, with amorphous and tetragonal forms predominating. It is generally accepted that a tetragonal phase is needed for catalytically active samples and that sulfated monoclinic zirconia exhibits poor activity in hydrocarbon isomerization reactions.[1]

In the current study, experimental and ab initio calculations have been performed with an aim of determining how the nature of the sulfate species is modified as a function of loading and how this later parameter influences the acidity and catalytic activity. For this purpose, a series of sulfated silica zirconia aerogels were prepared by in-situ and ex-situ procedures for samples where the Si/Zr ratio was held constant while the SO_4^{2-}/Zr ratio was varied over the range 0.2:1 to 0.3:1.

Experimental Section

Preparation. Sulfated 33 mol % zirconia−silica mixed oxides were prepared by modifying the method described by Yoldas to prepare xerogels.[17] TEOS (Silibond 90 wt %) was combined with water, propanol as a solvent, and nitric acid used as a hydrolysis catalyst. The above were combined in overall ratios of 1:1.2:1.5:0.2. The reagents were stirred under nitrogen for a 2 h prehydrolysis time, after which zirconium isopropoxide (70 wt %) diluted 10:1 in propanol was added such that the ratio of Si^{4+}/Zr^{4+} was 2:1. After a further hour, the final amount of hydrolysis water was added dropwise, and the final water/metal cation ratio was 2.6:1. All samples gelled within ∼3 days. Propanol was then exchanged for ethyl acetate via Soxhlet extraction for 5 h, and the ethyl acetate was then subsequently removed by supercritical drying. Initially the sample was left for 12 h in $scCO_2$ followed by a 30 min period of flushing every 2 h until no further ethyl acetate was detected in the effluent (typically after five flushes). Samples were then transferred to a tube furnace and calcined in flowing air at 873 K for 6 h. In-situ sulfated samples were prepared in a similar manner but using sulfuric acid in varying amounts as the hydrolysis catalyst, with the H^+ concentration being held constant by use of nitric acid. Ex-situ sulfation involved addition of appropriate amounts

10.1021/jp034190m CCC: $25.00
Published on Web 06/18/2003

TABLE 1: Absorption Coefficients and Acid Site Densities for Si−Zr Oxides of Varying Sulfate/Zirconium Ratios Produced by In-Situ and Ex-Situ Sulfation

sample	measured S content (wt %)	ϵ_{1540}[a]	ϵ_{1450}[a]	$n_{\text{Brønsted}}$[b]/nm^2	n_{Lewis}[b]/nm^2
SiZr (0)	0	0.53	1.78	0.217 (0.096)	0.161 (0.116)
SiZr (0.2-in)	1.54	0.77	2.08	0.279 (0.135)	0.202 (0.143)
SiZr (0.25-in)	2.13	0.66	1.74	0.253 (0.129)	0.204 (0.141)
SiZr (0.3-in)	3.00	0.64	1.98	0.274 (0.144)	0.191 (0.131)
SiZr (0.2-ex)	1.07	1.66	1.00	0.088 (0.049)	0.395 (0.266)
SiZr (0.25-ex)	1.84	1.18	1.11	0.121 (0.069)	0.374 (0.258)
SiZr (0.3-ex)	1.84	0.70	1.57	0.239 (0.133)	0.191 (0.134)

[a] IR absorption coefficient (cm μmol^{-1}). [b] Number of acid sites per nm^2, that is, number of base molecules retained per nm^2 after evacuation at 423 or 473 K.

of 0.01 M sulfuric acid to a precalcined aerogel followed by further calcination at 873 K.

Characterization. Surface acid densities were estimated using pyridine adsorption monitored by combined infrared spectroscopic and thermogravimetric techniques.[14] The infrared experiments were carried out using ~80 mg of sample pressed (at 0.10 tons cm^{-2}) into a 25 mm diameter disk. Spectra were recorded after the initial evacuation of the sample at 573 K and then after exposure to pyridine and evacuation at 423 and 473 or 488 K. Thermogravimetric analyses were carried out using a PC controlled CI microbalance attached to a conventional vacuum line fitted with rotary and oil diffusion pumps. Approximately 100 mg of sample as a fragmented pressed disk (prepared as per IR experiments) was evacuated for 2 h at 573 K and then exposed to 1 Torr pyridine and cooled to 373 K. A further 0.5 Torr of pyridine was introduced and the system allowed to equilibrate over 30 min. After this period, the sample was heated under vacuum to 423 K for 2 h and then at 473 K for 2 h while continually monitoring the mass. The mass due to retained pyridine following evacuation at the two temperatures, in combination with the integrated areas of the bands at ~1450 and 1540 cm^{-1} due to the 19b ring vibrations of pyridine adsorbed at Lewis and Brønsted sites, respectively, at the corresponding temperatures, allowed calculation of the respective absorption coefficients. The number of sites of each type was calculated by fitting the data to the equation

$$n_T = \frac{A_L C_d}{\epsilon_L m} + \frac{A_B C_d}{\epsilon_B m}$$

where n_T represents the total number of micromoles of pyridine per gram of sample adsorbed at each temperature, A is the integrated absorbance (cm^{-1}) of IR bands due to pyridine adsorbed at Lewis (L) or Brønsted (B) sites, C_d is the cross-sectional area (cm^2) of the pressed disk, m is the mass (g) of the pressed disk, and ϵ is the molar absorption coefficient (cm μmol^{-1}) for pyridine at Lewis (L) or Brønsted (B) sites. Combined IR−gravimetric experiments were repeated between three and five times to ensure the reproducibility of the values for each sample. The range of the calculated molar absorption coefficients fell within ±5.5% of the values presented in Table 1.

Activity Measurements. The liquid-phase reaction of styrene in toluene involved ~70 mg of catalyst which was calcined in dry air at 573 K, followed by addition of toluene (18 mL, Aldrich, 99.8%, HPLC grade, previously dried with a 5 A molecular sieve), without allowing the sample to contact ambient atmosphere. The sample in toluene was then transferred to the reactor containing styrene (17.3 mmol, Aldrich, 99%). The reaction was carried out in a 270 cm^3 steel autoclave fitted with a glass lining, a magnetically coupling stirred head, inlet/outlet ports, and a pressure measuring gauge. The autoclave was purged in N_2 and then heated in an oil bath to 333 K. After carrying out the reaction for 4.5 h and cooling to room temperature, the gases were vented and the composition of the solution was analyzed by gas chromatography using a 10% SP 2330 on Supelcoport column and a FID detector. A GC-MS (HP-6890, MSD HP-5973) fitted with a HP-5MS column was used to identify the reaction products.

The reaction products from the isomerization of but-1-ene were monitored using an on-line PE 8410 gas chromatograph fitted with a 0.19% picric acid on carbograph column of dimensions 2 mm × 2 m. The catalyst, typically 100 mg, was loaded into a vertically mounted fritted glass reactor and attached via Swagelok connections to a stainless steel line. The catalyst was calcined in dry air at either 573 or 773 K followed by cooling under nitrogen to 343 K. But-1-ene, controlled by a mass flow controller, was introduced at a rate of 1.2 mL min^{-1}, while nitrogen, at a rate of 90 mL min^{-1}, was used as a diluent. A sample of the effluent gas (2.5 μL) was injected into the column at 323 K after 10 min on stream.

Ab Initio Calculations. Ab initio calculations of model surface species were performed using the *Gaussian 98* program,[18] initially at the HF-SCF level and subsequently using the SCF-DFT method B3LYP. The latter incorporates Becke's three parameter hybrid functional[19] and the Lee, Yang, and Parr correlation functional[20] and generally gives superior results to those of HF-SCF calculations, which neglect the effects of electron correlation. All calculations were initially performed with the LanL2DZ basis set, which employs Dunning−Huzinaga double-ζ (DZ) basis functions[21] on first row elements and Los Alamos effective core potential with DZ functions on heavier atoms.[22] This effective core potential basis set was judged to be a reasonable compromise in view of the sizes of the species investigated, which contain two zirconium atoms. However, it proved that although B3LYP/LanL2DZ calculations yielded sensible zirconium−oxygen bond distances, the sulfur−oxygen bond distances were far from typical experimental values. Accordingly, a larger basis set was chosen, and although there is a strictly limited choice available for second row transition metals, the DZVP basis set of Godbout et al.[23] proved to yield credible results for molecular geometries and vibrational spectra.

Results

Table 1 shows the molar absorption coefficients obtained by combining the FTIR and gravimetric results for pyridine adsorption at several temperatures. As commented previously,[14] sulfated samples show a wide range of values for both the Lewis and Brønsted adsorbed forms although the values are much greater in the case of the ex-situ prepared samples. The availability of the molar absorption coefficients for each sample allowed the number of sites retaining adsorbate at various

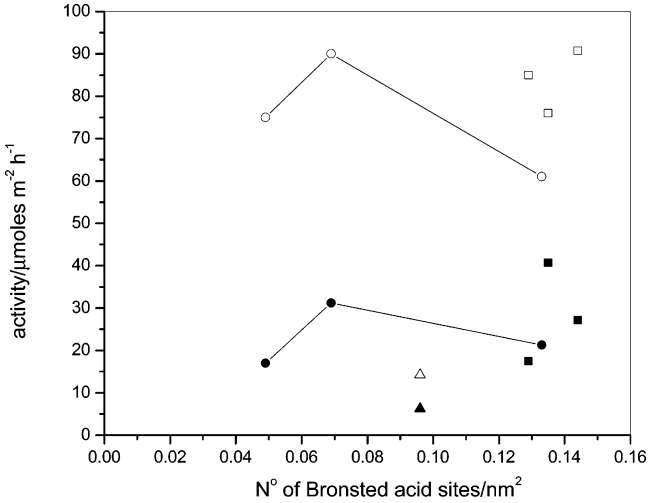

Figure 1. Activity data for but-1-ene isomerization at 348 K (open symbols) and reaction of styrene in toluene at 333 K (filled symbols) and the number of Brønsted acid sites which retained pyridine after 473 K evacuation for nonsulfated samples (triangles), in-situ sulfated samples (squares), and ex-situ sulfated samples (circles).

temperatures to be quantified. The number of Lewis and Brønsted acid sites which retained adsorbed base molecules at 423 and 473 K are also listed in Table 1. Ex-situ sulfated samples show a wider range of acid site densities and also show a trend of increasing Brønsted acid sites as a function of increased nominal sulfate loading at the expense of decreasing Lewis acid sites. On the other hand, the number of either type of acid site generated by the in-situ method appeared rather insensitive to the nominal sulfate loading.

Two catalytic test reactions were selected for the samples, one in the liquid and the other a gas-phase reaction. Both reactions and conditions were specifically selected to test only one type of acid site in order to determine whether correlation could be established with the number of sites available, as calculated by pyridine adsorption. Both toluene alkylation by styrene (and dimerization of styrene) and but-1-ene isomerization to *cis*- and *trans*-but-2-ene may be considered exclusively Brønsted catalyzed reactions under the conditions employed.[15,24,25] The *n*-alkane isomerization reaction, commonly used for sulfated zirconia catalysts, was not considered an appropriate test reaction due to controversy regarding whether redox processes are involved or whether particular Brønsted/Lewis acid site ratios may be significant.[5,6] Activities are shown in Figure 1, where the values have been plotted against the number of strong Brønsted acid sites which retained pyridine after evacuation at 473 K. Similar plots, with equivalent scatter of data, were obtained, however, when the *x*-axis was changed to the number of sites retaining pyridine after evacuation at lower temperatures. Although the nonsulfated silica−zirconia contained a significant number of Brønsted acid sites and was active in dimethyl acetal formation from methanol and acetone,[26] the sample was ineffective, in relative terms, in catalyzing either but-1-ene isomerization or toluene alkylation. Nonsulfated and sulfated samples all showed higher activity in the but-1-ene isomerization than in toluene alkylation. The in-situ sulfated samples, despite exhibiting similar acid site densities throughout the series (Table 1), did not all display the same levels of activity. Ex-situ sulfated samples, which exhibited a wide range of Brønsted acid site densities across the series, did not show a trend of increased activity with increasing site densities with a maximum activity corresponding with the sample SiZr (0.25-ex), which showed an intermediate level of Brønsted acid sites. A similar maximum

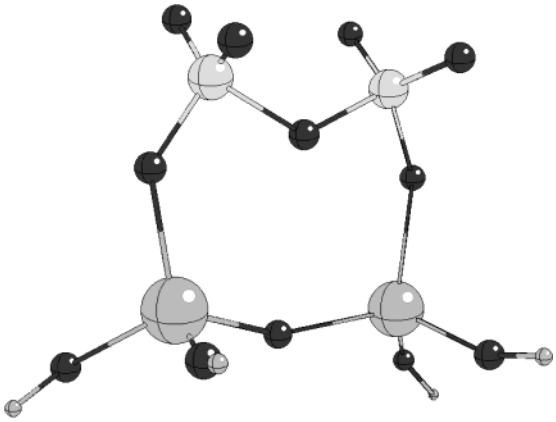

Figure 2. Optimized molecular geometry (B3LYP/DZVP) for the model of the dehydrated species.

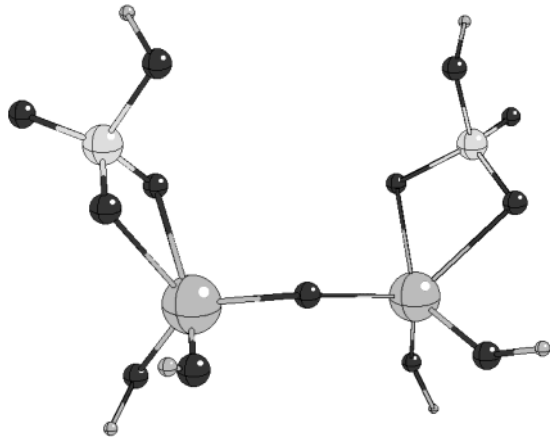

Figure 3. Optimized molecular geometry (B3LYP/DZVP) for the model of the hydrated species.

corresponding to this sample in activity plots for both reactions confirms that this sample was the most active of the series. Results in Figure 1 indicate that a common turnover frequency (TOF) does not exist for the samples and that not all sites detected by the probe molecule are of equivalent activity. The Brønsted acid sites for the 0.2 and 0.25 ex-situ sulfated samples were much more active than the sites present on the other samples.

To account for the range of activities shown by different sulfated samples, calculations were performed to analyze the different sulfated species which might exist under different reaction conditions. The optimized geometries of the models used to represent dehydrated and hydrated sulfated zirconia surfaces are shown in Figures 2 and 3, respectively. In both cases C_s symmetry was assumed, consistent with previous Raman spectroscopic measurements.[4] To avoid "open" valences on oxygen atoms, these were terminated with hydrogen atoms. This enabled the calculation to be performed on a neutral species, which is known to yield more sensible results than a calculation on an anion, which in our model would have necessitated a 4− charge. For anions it is generally necessary to include diffuse functions in the basis set in order to properly account for electrons relatively far from the nucleus. The addition of diffuse functions results in calculations which take far longer to compute. The hydrated species was initially represented by a model with four-coordinate Zr and monodentate sulfate with two S═O double bonds. However, during the geometry optimization the structure switched to five-coordinate Zr with bidentate sulfate, this arrangement having lower energy. Bond distances and interbond angles for the two models are

TABLE 2: Bond Distances (Å) and Interbond Angles (deg) Calculated for the Dehydrated and Hydrated Model Species

	dehydrated	hydrated
r(S═O)	1.446 ± 0.002	1.448
r(S−OS)	1.721	
r(S−OZr)	1.566	1.517
r(OH)		0.977
r(SO−Zr)	2.082	2.303 ± 0.015
θ(SOH)		108.3
θ(O═S═O)	122.0	
θ(O═S−O)	109.4 ± 1.8	114.5 ± 5.0
θ(O−S−O)	93.4	103.9 ± 2.0
θ(S−O−S)	126.7	
θ(S−O−Zr)	136.9	98.4 ± 0.5

TABLE 3: Calculated Band Positions and Assignments for the Sulfate Stretching Vibrations of the Dehydrated and Hydrated Model Species

$\tilde{\nu}$/cm^{-1}	potential energy distribution
	(a) Dehydrated
1391	96% ν(S═O) (a′)
1370	97% ν(S═O) (a″)
1192	89% ν(S═O) (a′)
1158	91% ν(S═O) (a″)
923	76% ν(S−OZr), 13% ν(ZrO) (a′)
905	58% ν(S−OZr), 32% ν(ZrO) (a″)
792	17% ν(S−O_{br}), 11% ν(S−OZr), 61% ν(ZrO) (a″)
678	26% ν(S−O_{br}), 11% ν(S−OZr), 31% ρ(SO_2) (a′)
621	52% ν(S−O_{br}), 17% δ(O−S−O) (a″)
	(b) Hydrated
3717	100% ν(OH) (a′)
3717	100% ν(OH) (a″)
1340	67% ν(S═O), 17% δ(SOH) (a′)
1337	67% ν(S═O), 17% δ(SOH) (a″)
1176	18% ν(S═O), 79% δ(SOH) (a′)
1173	19% ν(S═O), 17% δ(SOH) (a″)
1044	42% ν(S═O), 42% ν(S−OZr) (a′)
1038	44% ν(S═O), 40% ν(S−OZr) (a″)
989	45% ν(S═O), 32% ν(S−OZr) (a′)
985	41% ν(S═O), 35% ν(S−OZr) (a″)
796	75% ν(S−O) (a′)
783	72% ν(S−O), 11% ν(ZrO) (a″)

given in Table 2. The vibrational spectrum of each species was calculated at the optimized geometry. For computation of the potential energy distributions associated with the vibrational modes (Table 3), the Cartesian force constants and dipole derivatives obtained from the *Gaussian 98* output were converted to internal coordinates. These were used as the input to a normal coordinate analysis program derived from those of Schachtschneider.[27] Although it is often found that calculated force constants require scaling in order that calculated vibrational spectra match the experimental data, this was found to be unnecessary in the present case. Calculated IR spectra for the dehydrated and hydrated sulfated zirconia model species are shown in Figure 4.

The IR and Raman spectra of sulfated zirconia treated at 573 K display a broad band between 1400 and 1350 cm^{-1},[4,5,7,12] due to the ν(S═O) vibration of surface sulfate species. The broadness suggests that this may be the composite of at least two or three overlapping bands, and the calculations predict two ν(S═O) vibrations in this region for the hydrated species. In the ν(OH) region there is a band at 3761 cm^{-1} with a shoulder at 3737 cm^{-1}, where the calculations predict two ν(OH) bands at the same position (3717 cm^{-1}), with the one of a′ symmetry having greater intensity. There are a number of weak bands around 1600 cm^{-1}, which can be attributed to OH deformations, although calculations predict the δ(SOH) mode to be at lower wavenumber and strongly mixed with S═O stretching.

TABLE 4: Bond Distances (Å) and Interbond Angles (deg) Calculated for the Hydrated Model Species with Adsorbed Pyridine

	hydrated	adsorbed pyridine
r(S═O)	1.448	1.475
r(S−OZr)	1.517	1.543 ± 0.002
r(S−OH)		1.627
r(OH)	0.977	1.453
r(SO−Zr)	2.303 ± 0.015	2.258 ± 0.030
r(NH)		1.113
θ(SOH)	108.3	112.4
θ(O═S−O)	114.5 ± 5.0	112.3 ± 1.0
θ(O−S−O)	103.9 ± 2.0	106.5 ± 4.0
θ(S−O−Zr)	98.4 ± 0.5	98.8 ± 1.0
θ(O···N−H)		178.2

On treatment at progressively higher temperatures, the ν(OH) bands disappear, as conversion to the dehydrated form occurs. This is accompanied by a shift of the broad ν(S═O) band to ∼1390 cm^{-1}. This is fully in agreement with the calculated spectrum for the dehydrated species, which of course exhibits no ν(OH) bands other than those associated with OH groups attached to Zr. The latter are observed as a broad band around 3600 cm^{-1} which remains after treatment at higher temperatures. In the ν(S═O) region the dehydrated species is predicted to exhibit two bands, at 1370 and 1391 cm^{-1}, of which the latter (a′ symmetry) is predicted to be the stronger. It has not proved possible to distinguish ν(S−O) bands in the IR spectra because they are predicted to occur in the region below 1000 cm^{-1}, where there is strong IR absorption due to the oxide species and the calcium fluoride windows. These vibrations are predicted to shift to lower wavenumber upon dehydration.

It has previously been suggested[14] that the location of two (or more) adjacent sulfate species with active protons may lead to adsorbed pyridinium species at close proximity which might be responsible for the changes in molar absorption coefficient of the latter at high sulfate loading. A model species was then constructed for pyridine adsorbed on sulfated zirconia. In this model it was assumed that the hydroxyl groups on sulfur atoms function as Brønsted acidic sites, with protons transferred to adsorbed pyridine molecules. The optimized geometry is shown in Figure 5, with key bond distances and interbond angles listed in Table 4. It is evident that the adsorbed pyridinium ions remain close to the surface, hydrogen bonded to the SO_4^{2-} anionic sites. The vibrational spectrum of this model species was calculated; the IR spectrum is shown in Figure 6, and the band positions and assignments are listed in Table 5. Most of the strong bands in the 900−1700 cm^{-1} region are attributable to the pyridinium cation. These are all doubled, with a′ and a″ components, which have mostly identical wavenumber positions, indicating that there is no interaction between neighboring pyridinium ions. This is not surprising because in the model the nitrogen atoms are ∼10 Å apart.

The wavenumber of the S═O double bond stretch was significantly decreased upon interaction with pyridine, from 1340 to 1195 cm^{-1} for the a′ component. At the same time, the wavenumber positions of the S−O single bond stretching vibrations were all increased, by more than 100 cm^{-1}.

A calculation was also carried out on the dianion of the hydrated species in order to calculate the proton affinity. By subtracting the calculated energy of the dianion from that of the hydrated species, the proton affinity per proton was calculated to be 1351 kJ mol^{-1}. This value lies within the range calculated by Haase and Sauer.[10] Using the same method and basis set, we also calculated energies for H_2SO_4 and HSO_4^-, from which it was determined that the proton affinity for HSO_4^-

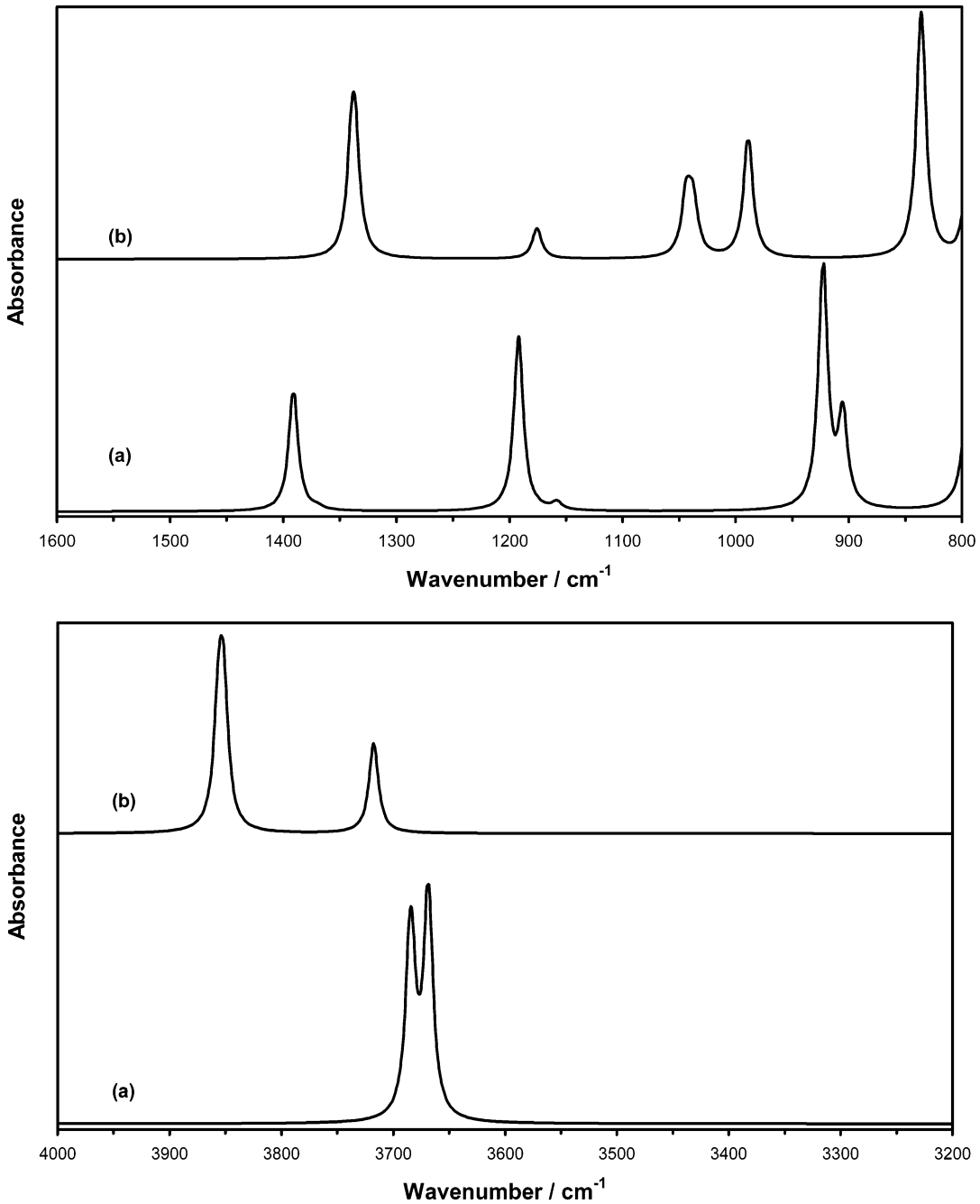

Figure 4. Calculated IR spectra (B3LYP/DZVP) for the models of the (a) dehydrated species and (b) hydrated species.

was 1312 kJ mol^{-1}. This indicates that the model species exhibits Brønsted acidity that is comparable with that of sulfuric acid.

Discussion

The incorporation of sulfate into a silica−zirconia mixed oxide leads to the generation of surface species which are capable of protonating but-1-ene, styrene, and pyridine. However, unlike the more widely studied sulfated zirconia, the sulfate-free silica−zirconia material alone presents Brønsted acid sites, as shown in this laboratory[13,25,26] and elsewhere.[7,15] Although Miller and Ko describe the sites on a similar 33 mol % ZrO_2-SiO_2 as being stronger than those on sulfated zirconia when calcined at 773 K,[15] results here show the unsulfated mixed oxide to have low activity in the protonation of the C═C group, despite the fact that it has a Brønsted acid site density in the same range as that of the sulfated materials. As some of the samples after sulfation exhibit lower Brønsted acid site densities than the nonsulfated materials (Table 1), it would appear that, at least to some extent, the addition of sulfate leads to formation of new, stronger sites at the expense of weaker protic sites present on the mixed oxide alone.

The absence of a straight line relationship between activity for either reaction normalized per unit surface area and the density of Brønsted acid sites (Figure 1) which would be indicative of a common turnover frequency for each reaction strongly suggests that a high degree of heterogeneity exists within a sample in terms of strength of the Brønsted acid sites. It could be suggested that the use of a relatively strong base such as pyridine overestimates the number of acid sites present. This would certainly be consistent with the high site density but low activities shown by the nonsulfated sample. Note that

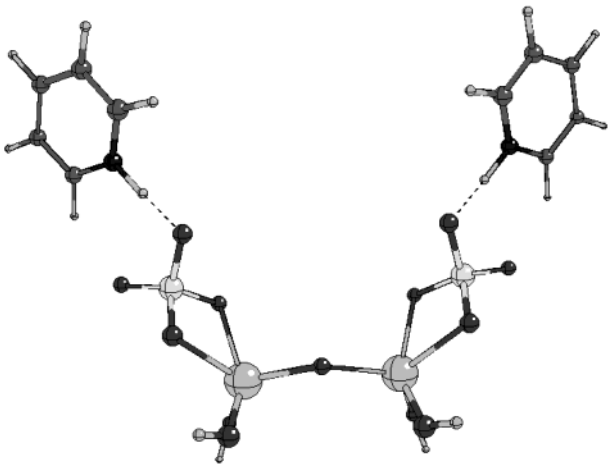

Figure 5. Optimized molecular geometry (B3LYP/DZVP) for the model of the hydrated species with adsorbed pyridine.

TABLE 5: Calculated Band Positions and Assignments for the Hydrated Model Species with Adsorbed Pyridine

a′		a″	
$\tilde{\nu}$/cm^{-1}	assignment	$\tilde{\nu}$/cm^{-1}	assignment
2069	ν(NH)	2055	ν(NH)
1707	δ_{ip}(NH) (a′)	1706	δ_{ip} (NH) (a″)
1674	8a (a′)	1674	8a (a″)
1602	8b (a′)	1602	8b (a″)
1518	δ_{ip}(CH) (a′)	1518	δ_{ip}(CH) (a″)
1448	δ_{ip}(CH) (a′)	1448	δ_{ip}(CH) (a″)
1376	δ_{ip}(CH) (a′)	1376	δ_{ip}(CH) (a″)
1323	14 (a′)	1323	14 (a″)
1229	δ_{ip}(CH) (a′)	1229	δ_{ip}(CH) (a″)
1195	ν(S═O) (a′)	1190	ν(S═O) (a″)
1193	δ(NHO) (a′)	1193	δ(NHO) (a″)
1178	δ_{ip}(CH) (a′)	1178	δ_{ip}(CH) (a″)
1090	19a (a′)	1090	19a (a″)
1084	19b (a′)	1084	19b (a″)
1072	ν(S−O) (a′)	1067	ν(S−O) (a″)
1038	1 (a′)	1038	1 (a″)
1030	δ_{op}(CH) (a′)	1030	δ_{op}(CH) (a″)
1019	δ_{op}(CH) (a′)	1019	δ_{op}(CH) (a″)
971	δ_{op}(CH) (a′)	970	δ_{op}(CH) (a″)
968	ν(O···H) (a′)	967	ν(O···H) (a″)
962	ν(S−OZr) (a′)	956	ν(S−OZr) (a″)
900	ν(S−OZr) (a′)	900	ν(S−OZr) (a″)

Miller and Ko, in describing a Brønsted acidity hierarchy for zirconia−silica−sulfate aerogels, placed the ability to irreversibly adsorb pyridine at 423 K above the ability to protonate but-1-ene at 423 K.[15] The fact that we still do not see a uniform TOF by using the amount of pyridine retained at 473 K at Brønsted acid sites suggests that the lack of correlation between activity and number of sites of a certain strength may be providing more information regarding the diverse types of site available on the surface of the sulfated mixed oxide. The variation in both Lewis and Brønsted molar absorption coefficients for the ex-situ sulfated samples (Table 1) would be consistent with this statement.

As mentioned above, the important parameters in securing activity of sulfate−zirconia systems are the calcination temperature of the nonsulfated zirconia precursor, the surface sulfate loading and the in-situ thermal activation of the sulfated zirconia. Each of these will be dealt with in the context of the following discussion.

The calcination temperature is of significance in sulfated zirconia systems with temperatures above 773 K required in order to form the active tetragonal form from the amorphous sulfated precursor.[5,28] The use of sulfated silica−zirconia adds an additional dimension in that the addition of silica is known to offset the crystallization of zirconia[13,15,29,30] and so temperatures above 773 K are required. It is possible that the addition of sulfate further delays the crystallization of zirconia by stabilizing the amorphous phase even though the initial addition of sulfate may enhance phase segregation by extracting zirconia to the surface of the mixed-oxide phase.[13] After 873 K calcination, the samples here were all X-ray amorphous.

Sulfuric acid is a strong acid, and it is clear that loss of the first proton occurs readily when in contact with an oxide surface. This effectively creates a Brønsted acid site where an exposed basic oxide anion accepts the proton to form a hydroxyl and leads to the loss of a Lewis acid site as a previously exposed zirconia cation ligates the HSO_4^- anion. Samples here (ex-situ series), in contrast, show an initial loss of Brønsted acid sites and an increase in Lewis acidity (Table 1) as a consequence of extraction of zirconia to the surface of the mixed oxide following acid catalyzed hydrolysis of the mixed-oxide linkages.[13] The loss of the second, much less acidic proton ($pK_a = 1.92$), depends on the availability of a second, adjacent base site of sufficient strength to accept the second proton. One may envisage that this particular geometric arrangement is not readily available and would be restricted to a small proportion of total zirconia sites which would be "titrated" by low concentrations of sulfate. Such completely deprotonated sulfate species would be present only at low sulfate loadings and would expose terminal S═O units, consistent with ab initio calculation studies of model surfaces[10] and with HRTEM studies.[8] There is some debate as to whether the completely deprotonated sulfate forms a bidentate surface species exposing two S═O units (6 coordinated S) or a tridentate species containing only one S═O unit (5 coordinated S),[1,8,10,31] although it is possible that a transformation from the former to the latter occurs around 800 K,[10] suggesting that differences in activation temperature may be the reason for the detection of one or the other. As indicated above and elsewhere,[1,31] such species are more likely to dominate at low sulfate coverage, possibly below 1.8 nm^{-1} exposed zirconia.[1,31]

The enhanced activity per unit site on ex-situ treatment at the lowest sulfation level of the silica−zirconia (Figure 1) indicates that a greater proportion of the sites available in the presence of the sulfate were capable of double-bond protonation. If it is assumed that these sulfate species are completely deprotonated at this low coverage, then the active Brønsted acid sites must be hydrogen terminated Zr or O^{2-} sites. However, as these new sites were created by a two-stage deprotonation of the sulfuric acid, it is possible that only sites created by transfer of the first proton are active, as the second stage of deprotonation must involve strong basic sites and thus generate relatively weak acid sites. Extraction of zirconia to the surface of the mixed oxide as a consequence of sulfuric acid catalyzed hydrolysis of mixed-oxide linkages[11,13,16] created a significant increase in Lewis acid sites, although, from the changes to the absorption coefficients of both Lewis and Brønsted bound pyridine (Table 1), both adsorbed forms were influenced by the presence of adsorbed sulfate (or by interaction with each other). It has been argued that the combination of adjacent Lewis sites and sulfate species is required for active samples.[6] If it was to be argued that the proximity of Lewis and Brønsted acid sites to the sulfate unit was responsible for the significant modifications to both absorption coefficients (Table 1), then one would have to assume that the Lewis and Brønsted acid sites on the in-situ sulfated samples were not influenced by the presence of the sulfate unit, as these exhibited absorption coefficients akin

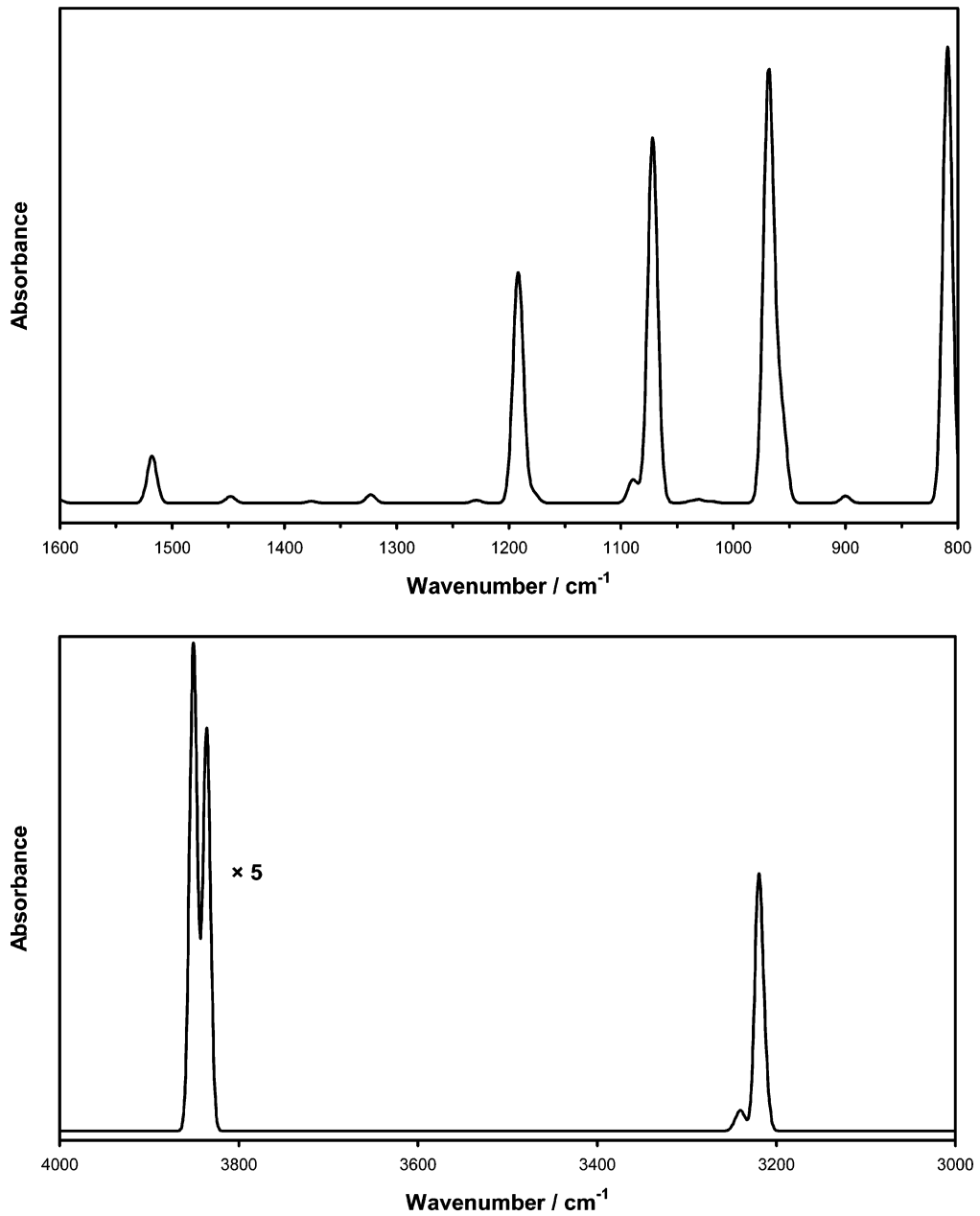

Figure 6. Calculated IR spectrum (B3LYP/DZVP) for the model of the hydrated species with adsorbed pyridine.

to those of the parent mixed oxide (Table 1). This sample generated a high density of Brønsted acid sites even at low sulfate loadings but did not display the corresponding high activity predicted (Figure 1). It has previously been suggested[13] that the in-situ series of sulfated samples show minimal variation of acid site densities as a function of sulfate loading, as they have lower surface levels of amorphous zirconia which therefore contain regionally high sulfate densities. This high density of sulfate, even at low overall sulfate loadings, would limit the number of adjacent Lewis sites available and consequently place the two types of adsorption site at such distances apart that the adsorbed pyridine on the two types of site would not interact and consequently they would not mutually modify each others' absorption coefficients for adsorbed pyridine (Table 1).

Low sulfate loadings, on the other hand, for the ex-situ sulfated samples, probably involve isolated sulfate units, with the low coverage of amorphous zirconia allowing for the presence of high (Table 1) Lewis acid densities and the potential to locate both Brønsted and Lewis forms of adsorbed pyridine in such close proximity that the two adsorbed forms mutually modify each others' absorption coefficients (Table 1). At the lowest sulfate loading in both series, significantly greater densities of Brønsted acid sites are created for the in-situ than for the ex-situ series (Figure 1) and yet this enhanced Brønsted acid site density did not manifest itself in terms of significantly greater catalytic activity for either test reaction (Figure 1). One possible explanation, which we will return to throughout the discussion, is the scenario that high activity in a proton catalyzed reaction whose initial stage involves activation of a molecule containing a C═C depends not only on the Brønsted acid site density (assuming sites of suitable strength are present) but also on the presence of an adjacent Lewis acid site at which the interaction between the π electrons of the double bond and the Lewis acid site acts as a "docking site" prior to protonation. Such a proposal, involving the need for both types of acid site in close proximity, would explain why we do not observe straight line relationships between Brønsted acid site densities and catalytic activity for either of our chosen reactions (Figure 1). We have previously argued that, in the case of toluene reaction with styrene over silica−zirconia supported heteropoly

acid catalysts,[25] the competing alkylation and dimerization reactions depend on the relative surface concentrations of the two molecules and that the most likely sites involved are Lewis acid sites of the exposed zirconia. In such a case, activity to one product would not be expected to depend only on the Brønsted acid site density. If such a scenario is in fact correct and both Brønsted and Lewis acid sites are required, then the model must hold as sulfate loadings are increased and continued modifications to both site densities and absorption coefficients of adsorbed molecules are observed (Table 1). This will be shown over the remainder of the discussion.

Increasing the sulfate loading (to 0.25 sulfate:1 zirconium) increased the Brønsted acid site density at the expense of Lewis acid sites for the ex-situ samples (Table 1), suggesting that "titration" of the latter type of site by sulfate had occurred. On the other hand, a slight loss in Brønsted acidity for the in-situ series was not balanced by a loss in Lewis sites, which remained essentially constant (Table 1). This slight loss in Brønsted acid sites did, however, give rise to more significant changes in activities for both reactions, again suggesting that the Brønsted acid site density alone is not sufficient to determine activity. Enhanced Brønsted acidity for the 0.25 ex-situ prepared sample was matched by an increase in activity which was mirrored in both reactions (Figure 1). The observation that for this sample the absorption coefficients for adsorbed pyridine were perturbed from the average values of 1.24 and 1.56 cm μmol^{-1} at 1540 and 1450 cm^{-1}, respectively,[14] observed for a range of samples, would suggest the location of both forms of adsorption site at sufficiently close proximity to allow mutual interactions.

As the sulfate loading was increased to its highest level (0.3 sulfate:1 zirconium), the density of groups, assuming that sulfate is only located on the zirconia component,[15] reaches levels for which polysulfates are expected.[2,31] Although such species have been proposed for sulfated zirconia,[2,31,32] these have been envisaged as bidentate units with each sulfur carrying only one double bond to oxygen. Given the preference shown by the pyrosulfuric acid molecule for coordination of six, a structure containing a single bond to the zirconia surface and two double bonds to oxygens is suggested here (Figure 2). The presence of such an adsorbed pyrosulfate species makes it quite clear why the in-situ pretreatment temperature is thought to be so crucial,[1,2,6,32] since the addition/removal of water will control the extent of hydrolysis of such a species to produce a hydrated form, as shown in Figure 3. Hydrolysis of the pyrosulfate to produce two sulfate units each with an available proton of calculated affinity energy of 1351 kJ mol^{-1} should be capable of adsorption of pyridine in its pyridinium form (Figure 5). It has previously been suggested that the proximity of the two adsorbed ring structures on such surface sulfate species may be responsible for the modifications observed to the molar absorption coefficient observed for the pyridinium ion vibration at 1540 cm^{-1}.[14] However, the model calculations predict the nitrogen atoms to be spaced at ∼10 Å apart and the calculated components of the spectra are doubled, with a′ and a″ components, which have mostly identical wavenumber positions (Table 4), again indicating that there should be no interaction between neighboring pyridinium ions. Note that the addition of further sulfate units in the vicinity of the adsorbed pyrosulfate might influence the extent to which each pyridine ring might lean over to reduce ring−ring interaction. However, the model structure (Figure 5) would predict that, even in such a case where the rings might be pushed into a vertical position, placing them parallel to each other, the distances between each ring would be unlikely to be reduced below the 10 Å calculated for the N distances. Additionally, although the electronic interactions between two adjacent adsorbed pyridinium rings would account for the lowering of the molar absorption coefficient for the 1540 cm^{-1} band for the highest sulfate loaded samples,[13] such a scenario would not explain the mutual influence that the Brønsted and Lewis adsorbed forms of pyridine appear to have in terms of the modification of the molar absorption coefficients for both species (Table 1). Such a scenario can only be envisaged when both Lewis and Brønsted bound forms are located as neighbors due to the presence of adjacent adsorption sites, an arrangement which we propose would be beneficial in terms of the initial adsorption and then protonation of vinyl group containing molecules. Such an arrangement is apparently optimized for the SiZr (0.25 ex) sample which displays (Figure 1) the maximum TOF when calculated in terms of the number of Brønsted acid sites which it possesses. The fact that other samples possess a greater number of these sites but display either lower, equivalent, or, at most, marginally improved activity (Figure 1) supports our proposal that high Brønsted site density alone is not sufficient to provide high activity. Increasing the sulfate loading from 0.25 SO_4^{2-}/Zr to 0.3 SO_4^{2-}/Zr for the ex-situ series increased the density of Brønsted acid sites (Table 1). When the density of retained surface sulfate is calculated in terms of the unit area of exposed (surface) zirconia,[13] this equates to the formation of one additional Brønsted acid site for each additional sulfate unit added. Such data would be entirely consistent with the conversion of the isolated sulfate units into the pyrosulfate species depicted in Figure 3, assuming that the moisture levels are sufficient[6] to ensure that a hydrated form is present. This increased Brønsted acid site density did not lead to enhanced activity in either toluene alkylation or double bond isomerization of but-1-ene, and in fact, activity decreased in both reactions at this loading. Again, this might be justified from our model involving the participation of both Lewis and Brønsted acid site pairs in alkene activation. Although the addition of each additional sulfate unit created an additional Brønsted acid site, the consumption of previously exposed zirconia displaying Lewis acidic characteristics must be considered. Again, on the basis of sulfate density per unit exposed zirconia,[13] data in Table 1 suggest that each additional sulfate group, in addition to generating an additional Brønsted acid site, leads to the loss of 1.5 Lewis acid sites.

Sulfated zirconia (rather than the silica−zirconia employed here) has been extensively studied[1−3,33−35] for the isomerization of light alkanes leading to branched isomers. Controversy still exists as to whether strong acidity alone is sufficient or whether a role exists involving redox processes.[6] In terms of acidity, some authors[6,33] believe that the presence of both Lewis and Brønsted acid sites is required in order to generate "superacidity". Morterra et al.[34] have stated that a relationship between Brønsted acid sites and activity for isomerization of light alkanes is unlikely and that[35] Lewis acidity plays a dominant role. In view of the apparent necessity for both types of center,[33−35] some authors have taken to presenting data in the form of Lewis/Brønsted (L/B) acid site ratios.[5,33] It is unlikely that such a relationship might be related to correlate with catalytic behavior, for the following reasons:

(a) Increased L/B ratios may derive from increased Lewis density or decreased Brønsted acid density and provide no indicator of the optimum ratio.

(b) L/B ratios give no indication of the relative proximity of sites.

(c) L/B ratios based on densities calculated from base molecule adsorption tend[14] to use literature values for molar

absorption coefficients which assume constant values irrespective of the sulfate loading.

Results here for sulfated silica−zirconia tested in reactions involving protonation of a C=C suggest that both Lewis and Brønsted acid site pairs are required for activation, as observed for isomerization of light alkanes.[1,6,33,35] However, the calculation of total densities does not provide correlation with activity, as neighboring pairs are most likely involved in the active site arrangement. In the present paper, some indication of the proximity of Brønsted and Lewis sites has been derived by the manner in which the molar absorption coefficients of adsorbed pyridine have been perturbed when these adsorption sites are sufficiently close.

Acknowledgment. We wish to thank the University of Dundee for a University scholarship (to D.J.R.) and the EU for a Marie Curie Fellowship (to B.B.-B.).

References and Notes

(1) Morterra, C.; Cerrato, G.; Pinna, F.; Signoretto, M. *J. Catal*. **1995**, *157*, 109.

(2) Morterra, C.; Cerrato, G.; Pinna, F.; Signoretto, M. *J. Phys. Chem*. **1994**, *98*, 12373.

(3) Clearfield, A.; Serrette, G. P. D.; Khazi-Syed, A. H. *Catal. Today* **1994**, *20*, 295.

(4) Reimer, T.; Spielbauer, D.; Hunger, M.; Mekhemer, A. H.; Knözinger, H. *J. Chem. Soc., Chem. Commun*. **1994**, 1181.

(5) Morterra, C.; Cerrato, G.; Ardizzone, S.; Bianchi, C. L.; Signoretto, M.; Pinna, F. *Phys. Chem. Chem Phys*. **2002**, *4*, 3136.

(6) Song, S. X.; Kydd, R. A. *J. Chem. Soc., Faraday Trans*. **1998**, *94*, 1333.

(7) Navío, J. A.; Colón, G.; Macías, M.; Camplelo, J. M.; Romero, A. A.; Marinas, J. M. *J. Catal*. **1996**, *161*, 605.

(8) Benaïssa, M.; Santiesteban, J. G.; Díaz, G.; Chang, C. D.; José-Yacamán, M. *J. Catal*. **1996**, *161*, 694.

(9) Babou, F.; Bigot, B.; Sautet, P. *J. Phys. Chem*. **1993**, *97*, 11501.

(10) Haase, F.; Sauer, J. *J. Am. Chem. Soc*. **1998**, *120*, 13503.

(11) Jung, S. M.; Dupont, O.; Grange, P. *Appl. Catal. A* **2001**, *208*, 393.

(12) Barthos, R.; Lónyi, F.; Engelhardt, J.; Valyon, J. *Top. Catal*. **2000**, *10*, 79.

(13) Rosenberg, D. J.; Coloma, F.; Anderson, J. A. *J. Catal*. **2002**, *210*, 218.

(14) Rosenberg, D. J.; Anderson, J. A. *Catal. Lett.* **2002**, *83*, 59.

(15) Miller, J. B.; Ko, E. I. *Chem. Eng. J.* **1996**, *64*, 273.

(16) Lopez, T.; Tzompantzi, F.; Navarrete, J.; Gomez, R.; Boldú, J. L.; Muñoz, E.; Novaro, O. *J. Catal*. **1999**, *181*, 285.

(17) Yoldas, B. E. *J. Non-Cryst. Solids* **1980**, *38*, 81.

(18) Frisch, M. J.; Trucks, G. W.; Schlegel, H. B.; Scuseria, G. E.; Robb, M. A.; Cheeseman, J. R.; Zakrzewski, V. G.; Montgomery, J. A., Jr.; Stratmann, R. E.; Burant, J. C.; Dapprich, S.; Millam, J. M.; Daniels, A. D.; Kudin, K. N.; Strain, M. C.; Farkas, O.; Tomasi, J.; Barone, V.; Cossi, M.; Cammi, R.; Mennucci, B.; Pomelli, C.; Adamo, C.; Clifford, S.; Ochterski, J.; Petersson, G. A.; Ayala, P. Y.; Cui, Q.; Morokuma, K.; Malick, D. K.; Rabuck, A. D.; Raghavachari, K.; Foresman, J. B.; Cioslowski, J.; Ortiz, J. V.; Stefanov, B. B.; Liu, G.; Liashenko, A.; Piskorz, P.; Komaromi, I.; Gomperts, R.; Martin, R. L.; Fox, D. J.; Keith, T.; Al-Laham, M. A.; Peng, C. Y.; Nanayakkara, A.; Gonzalez, C.; Challacombe, M.; Gill, P. M. W.; Johnson, B.; Chen, W.; Wong, M. W.; Andres, J. L.; Gonzalez, C.; Head-Gordon, M.; Replogle, E. S.; Pople, J. A. *Gaussian 98*, Revision A.5; Gaussian, Inc.: Pittsburgh, PA, 1998.

(19) Becke, A. D. *J. Chem. Phys*. **1993**, *98*, 5648.

(20) Lee, C.; Yang, W.; Parr, R. G. *Phys. Rev. B* **1988**, *37*, 785.

(21) Dunning, T. H.; Hay, P. J. In *Modern Theoretical Chemistry*; Schaefer, H. F., III, Ed.; Plenum: New York, 1976; Vol. 3, p 1.

(22) Hay, P. J.; Wadt, W. R. *J. Chem. Phys*. **1985**, *82*, 270, 284, and 299.

(23) Godbout, N.; Salahub, D. R.; Andzelm, J.; Wimmer, E. *Can. J. Chem*. **1992**, *70*, 560.

(24) Goldwasser, J.; Engelhardt, J.; Hall, W. K. *J. Catal*. **1981**, *71*, 381.

(25) Bachiller-Baeza, B.; Anderson, J. A. *J. Catal*. **2002**, *212*, 231.

(26) Anderson, J. A.; Fergusson, C. A.; Rodríguez-Ramos, I.; Guerrero-Ruiz, A. *J. Catal*. **2000**, *192*, 344.

(27) Shachtschneider, J. A. *Vibrational Analysis of Polyatomic Molecules*, Parts V and VI; Technical Report Nos. 231 and 57; Shell Development Co.: Houston, TX, 1964 and 1965.

(28) Morterra, C.; Cerrato, G.; Signoretto, M. *Catal. Lett*. **1996**, *41*, 101.

(29) Navío, J. A.; Marchena, F. J.; Macías, M.; Colón, G.; Avilés, M. A.; Sánchez-Soto, P. J. *J. Sol−Gel Sci. Technol*. **1997**, *10*, 165.

(30) Aguilar, D. H.; Torres-Gonzalez, L. C.; Torres-Martinez, L. M.; Lopez, T.; Quintana, P. *J. Solid State Chem*. **2000**, *158*, 349.

(31) Bensitel, M.; Saur, O.; Lavalley, J. C.; Morrow, B. A. *Mater. Chem. Phys*. **1988**, *19*, 147.

(32) Morterra, C.; Cerrato, G.; Bolis, V. *Catal. Today* **1993**, *17*, 505.

(33) Nascimento, P.; Akratopolou, C.; Oszagyan, G.; Coudurie, G.; Travers, C.; Joly, J. F.; Vedrine, J. C. In *New Frontiers in Catalysis*; Gutzi, L., Solymosi, F., Tetenyi, P., Eds.; Akademiai Kiado: Budapest, 1993; Vol. B, p 1185.

(34) Morterra, C.; Cerrato, G.; Pinna, F.; Signoretto, M.; Strukul, G. *J. Catal*. **1994**, *148*, 181.

(35) Pinna, F.; Signoretto, M.; Strukul, G.; Cerrato, G.; Morterra, C. *Catal. Lett*. **1994**, *26*, 339.